Airborne Measurements of Arctic Sea Ice, Glacier and Snow Emissivity at 24-183 GHz

Tim J.Hewison[1], Nathalie Selbach[2], Georg Heygster[2], Jon P.Taylor[1] and Andrew J.McGrath[1]

[1]Met Office, UK [2]University of Bremen, Germany

***Abstract*--Microwave radiometers were operated on a research aircraft during low-level flights in the Arctic in March 2001. Data from these instruments are used to calculate surface emissivity at millimetre wavelengths. This calculation includes the retrieval of an effective temperature from multiple channels centred at 183 GHz. Emissivity spectra will be presented for a range of surface types, including open water, new ice (nilas), first year, multi-year, and glacial ice. These show that the emissivity of older ice types is lower at 24 GHz, decreases further at higher frequencies, but usually starts to increase by 157 or 183 GHz. These results will help exploit data from satellite instruments, such as AMSU, in the Arctic.**

I. Introduction

The application of satellite data from microwave radiometers, in the arctic is currently limited by our knowledge of the surface emissivity. This is highly variable and difficult to estimate from space-borne observations, due to the uncertainty in the atmospheric absorption and surface temperature.

An example application is the retrieval of low values of Total Water Vapour (TWV) using data from the 183 GHz channels of AMSU or SSM/T-2 [1]. This algorithm relies on these channels having the same surface emissivity. However, it can be extended to higher values of TWV by including data from the 150 GHz channel, but this requires knowledge of how the surface emissivity varies over this spectral range.

II. The POLEX-SEPOR experiment

The Met Office conducted an airborne campaign, POLEX-SEPOR, (Polar Experiment - Surface Emissivity in Polar Regions) in March 2001 to measure the emissivity of various arctic surfaces, based in Tromsø, Norway. Previous work [2] concentrated on the Baltic Sea, where ice formations are quite different due to the low salinity and lack of multi-year ice. Since then, new channels at 183 GHz and an infrared interferometer, *ARIES*, have been added to the aircraft.

A. Instrumentation

Microwave radiometers, known as Deimos and MARSS were operated on a C-130 aircraft. These are total power radiometers, both with a 3 s along-track scan, which includes various views downward, and upward for MARSS. The characteristics of these instruments during this experiment are given in Table 1. They are described in detail in [3] and [4].

TABLE 1 - CHARACTERISTICS OF MICROWAVE RADIOMETERS DURING POLEX

Instrument	Deimos		MARSS				
AMSU Channel	1	3	16	17	18	19	20
Frequency (GHz)	24	50	89	157	183 ±1	183 ±3	183 ±7
View angles along track	Down only +35° to -5°		Up and Down +40° to -40°				
Beamwidth (FWHM)	11°	11°	12°	11°	6°	6°	6°
Sensitivity NEΔT (K)	0.6	0.6	0.5	0.7	0.6	0.4	0.3
Cal. Acc. (K)	3	3	0.9	1.1	1.0	0.9	0.8

The aircraft was also equipped with an infrared radiometer to measure the skin temperature, an infrared interferometer, *ARIES,* a short-wave spectrometer, hemispherical pyranometers and pyrgeometers, video cameras and a wide range of supporting meteorological sensors.

B. Flights

Five flights of up to 10 hours duration were flown over various types of arctic sea ice and glaciers in the Svalbard area of the Barents and Greenland Seas. Three of these flights extended to 85° N, to sample first year and multi-year ice, including runs over glacial ice on Svalbard. The other two concentrated on the Marginal Ice Zone. Each flight comprised of a long run at low level (150 m or 600 m above mean sea level), a profile ascent, and a return leg at high level (8.5 km) back along the same track. Dropsondes were released at about 100 km intervals on the return leg to provide atmospheric profiles along the track, which are used to validate the total water vapour retrievals [1].

On all flights, there was a northerly airflow, which resulted in cloud-free conditions over the ice, but convective cloud developed over open water. The surface temperature got as low as -50 °C, and the surface inversion trapped a variable concentration of ice crystals.

One additional, shorter sortie was flown to measure the emissivity of snow-covered forest. This consisted of a series of low-level runs near Sodankylä in northern Finland. The sky was free of cloud in the operating area.

III. Emissivity Calculation

A. Definition of emissivity

Measured brightness temperatures must be converted to surface emissivity to extend them to general application. However, even the definition of emissivity introduces potential ambiguities unless it is carefully defined. These aspects are discussed below.

This emissivity calculation assumes surface reflection to be purely specular, as this is consistent with the treatment used for the sea surface in fast radiative transfer models. However, most snow and ice surfaces are close to Lambertian.

Equation (1) is used to calculate the emissivity using only aircraft data:

$$e(\nu,\theta) = \frac{T_n(\nu,\theta) - T_z(\nu,\theta)}{T_s - T_z(\nu,\theta)} \quad (1)$$

where $e(\nu,\theta)$ is the emissivity at frequency, ν, and incidence angle, θ, and T_n are T_z the up- and downwelling brightness temperatures at the surface, respectively, and T_s is the surface (skin) temperature. The calculation of each of these terms is discussed below.

B. Modelling downwelling radiances for Deimos

Downwelling brightness temperatures at Deimos frequencies are needed to calculate emissivity, but are not directly measured. However, they are not expected to vary significantly. Absorption at 24 GHz is weak due to the very low water vapour levels. Absorption at 50 GHz is dominated by oxygen, which does not vary greatly. Analysis of dropsonde profiles reveals the temperature of the atmosphere above the aircraft remained relatively constant during each flight. This allows a single dropsonde to be used to represent the atmospheric profile above the aircraft for each flight. This profile is used as input to a radiative transfer model [5] to predict the downwelling brightness temperatures that would be measured by Deimos. These values are expected to be accurate to better than 0.5 K in cloud-free conditions.

C. Correcting atmospheric absorption below the aircraft

The atmosphere below the aircraft will affect the measured brightness temperatures by absorption and emission (scattering is neglected, as there must be no cloud below the aircraft for surface observation). When calculating emissivity, it is necessary to know the brightness temperatures at the surface, so corrections must be applied to aircraft measurements of both down- and up-welling brightness temperatures.

The atmosphere below the aircraft at any time is assumed to be vertically homogeneous. The average pressure between the flight level and the surface is used. Analysis of the dataset of dropsonde profiles shows that the mean temperature of the atmosphere below the aircraft, $\overline{T}$, can be modelled as a polynomial function of the air temperature at the flight level, T_{FL} and the surface temperature, T_S (from dropsonde) with an rms accuracy of 0.6 K using equation (2):

$$\overline{T} = T_s - 0.26 + 0.519\cdot(T_{FL} - T_s) - 0.015\cdot(T_{FL} - T_s)^2 + 0.0013\cdot(T_{FL} - T_s)^3 \quad (2)$$

The mean humidity of the atmosphere below the aircraft, $\overline{q}$ can be modelled in a similar way based on the humidity at the flight level, q_{FL} and the surface, q_s, assuming it is saturated at the surface (3). This was found to predict $\overline{q}$ with an rms accuracy of 7%.

$$\overline{q} = q_s - 0.60\cdot(q_{FL} - q_s) \quad (3)$$

These mean values for the pressure, temperature and humidity of the atmosphere below the aircraft input to a radiative transfer model [5], which is used to predict the absorption at a single representative frequency for each channel. The frequencies are given in Table 2.

TABLE 2 - Effective Frequencies used in Radiative Transfer Model

	Deimos		MARSS				
AMSU Channel	1	3	16	17	18	19	20
Effective Frequency (GHz)	23.8	50.1	88.9	157.5	182.4	180.4	176.8

The atmospheric correction scheme can be validated by examining the observed and corrected downwelling brightness temperatures during a profile ascent in clear skies. This produced an rms difference between the corrected values at 600m and the surface of typically 0.2K for Deimos and 1K for MARSS. The uncertainty introduced in the atmospheric correction scheme dominates the accuracy of the emissivity at 183 GHz from 600m.

The overall uncertainty in the emissivity retrieved from low-level aircraft data by this method is estimated to be ±0.010 for e=0.900 at 183±7 GHz. This is dominated by uncertainty in absolute brightness temperatures at the surface, due to the correction for atmospheric absorption.

IV. Surface Temperature

To calculate emissivity (1), it is necessary to know the surface temperature. This can be estimated in a number of ways described in this section. The resulting emissivity depends on the definition of surface temperature, so it is important to consider the application. In our case, it is to provide a background for retrieving atmospheric information from satellite instruments.

A. Infrared radiometer - Heimann

The Heimann KT19.82 is a thermal infrared radiometer with a fixed downward view, which it samples continuously at 4 Hz. Its broad bandwidth (8-15 μm) provides a "dirty window" in which it measures brightness temperature. Its measurements need to be corrected for atmospheric absorption. The optical depth, τ_{IR} can be modelled using (4):

$$\tau_{IR} = 0.142 \cdot (\bar{q} \cdot h)^{0.38} \quad (4)$$

Where $\bar{q}$ is the mean humidity (kg/kg) of the atmosphere below the aircraft from (3), and h is the aircraft height (m). The coefficients in (4) were derived by regression of the modelled transmittance over the Heimann passband over a range of high-latitude atmospheres. It was found to predict τ_{IR} with an rms of 5%. This scheme typically produces corrections of the order of +1K over open water and -1K over colder ice surfaces from an altitude of 300m in arctic atmospheres. Again, the accuracy of this correction is limited by uncertainty in $\bar{q}$, which is estimated to be ± 20% at 300m.

Allowance should also be made for surfaces with an infrared emissivity of less than 1. This will introduce a bias in the measurement of surface temperature which, in turn, will bias the resultant microwave emissivity. So the brightness temperatures measured by the Heimann need to be further corrected by a factor, which depends on the downwelling infrared flux and the surface emissivity. The infrared emissivity of snow and ice surfaces is the subject for ongoing research [6]. Initial results suggest the average emissivity over 800-1200 cm^{-1} is 0.97 for thick, old sea ice and 0.99 for snow covered land. These figures suggest the skin temperature of sea ice is between 0.2-1.2 K higher than the Heimann brightness temperature (after atmospheric correction). The corrections are correspondingly smaller for snow surfaces. However, these corrections have not been applied to the data, pending confirmation of the infrared emissivity study.

B. Infrared interferometer - ARIES

Another approach is to retrieve skin temperature and surface emissivity from a combination of up- and down-welling radiance spectra measured in the thermal infrared by ARIES [6]. Initial results show the retrieved skin temperature agrees within ±1K of the uncorrected brightness temperature measured by the Heimann radiometer over sea ice. It may be fortuitous that the corrections for atmospheric absorption and infrared emissivity needed for the Heimann tend to cancel out in this case. This has been taken as validation of the accuracy of the Heimann measurements. These will be used in preference to ARIES retrievals, despite their reduced accuracy, to improve on the sporadic coverage provided by ARIES.

C. Retrieving from microwave radiometer

Although we can measure the skin temperature using infrared radiometers, microwaves penetrate some distance into snow and ice surfaces, due to the weak absorption of microwaves by ice. Snow pack consists of ice crystals suspended in a medium of air. Sea ice is also an inhomogeneous medium - depending on the ice type, it contains air and brine pockets of different sizes. The penetration depth depends on the wavelength, the size and composition of inhomogeneities within the medium. Typically, the penetration depth is ~10 wavelengths in ice, and ~100 wavelengths in dry snow at AMSU frequencies.

Sea ice has low thermal conductivity. Multi-year ice can support a linear temperature gradient of ~50K across a 4 m thickness above water at ~ 1.8 °C. Assuming a linear thermal gradient, 24 GHz will penetrate 1.25 m into the ice, where the temperature is 15K warmer than the surface, but 183 GHz would only be expected to see to a depth where the temperature is 2K warmer than the surface. The thermal conductivity of snow is ~8 times lower than sea ice, but the problem is further complicated by its unknown thickness and the temperature of the underlying surface.

It is possible to retrieve the *effective temperature* for microwave emissions from MARSS observations. The surface emissivity is assumed to be the same for all 3 channels centred on the 183 GHz water vapour line. This allows simultaneous measurements by these channels to be used to derive the emissivity and effective temperature. This is implemented by minimising a Cost Function , C, describing the squared difference between the observed nadir brightness temperatures, T_n^{OBS} , and those from the Radiative Transfer Equation, T_n^{RTE}:

$$C = \sum_{ch} \left(T_n^{OBS} - T_n^{RTE} \right)^2 \qquad ch = 183 \pm 1, \pm 3, \pm 7 \; GHz \quad (5)$$

The Cost Function, C, is minimised by differentiating with respect to the emissivity, e_{183}, and effective temperature, T_{eff}, in the Radiative Transfer Equation and solved to find best estimates of these parameters. All the 183 GHz channels are included in the cost function, if the atmosphere below the aircraft is optically thin ($\tau < 1$), which was usually the case below ~1km during this experiment.

$$\frac{\partial C}{\partial e_{183}} = 0 \quad and \quad \frac{\partial C}{\partial T_{eff}} = 0 \quad (6)$$

This effective temperature is generally higher than the skin temperature measured by the infrared radiometer by ~18 K over snow covered land, ~12 K over multi-year ice, ~8 K over thick first year ice, but <~5 K over thin new ice. This difference over multi-year ice is several times larger than expected, which may be explained using an exponential temperature profile in the ice. An alternative explanation is that this difference is due to snow cover, which has a very low thermal conductivity.

The effective temperature retrieved from MARSS' 183 GHz channels is used to calculate the emissivity for all other MARSS and Deimos channels. Although lower frequencies have a greater penetration depth, this is still felt to be more appropriate than using an IR skin temperature. It has the additional advantage of preventing the emissivity calculated at low frequencies exceeding 1, which is unphysical. It remains to be seen whether the effective temperature can be retrieved in a similar way from satellite measurements. This would be required to apply the emissivities presented here to the operational assimilation of satellite data.

This method has the additional advantage over the IR skin temperature of being insensitive to scattering by small ice crystals often found in the surface inversions. Extinction of this type is difficult to correct for in infrared measurements.

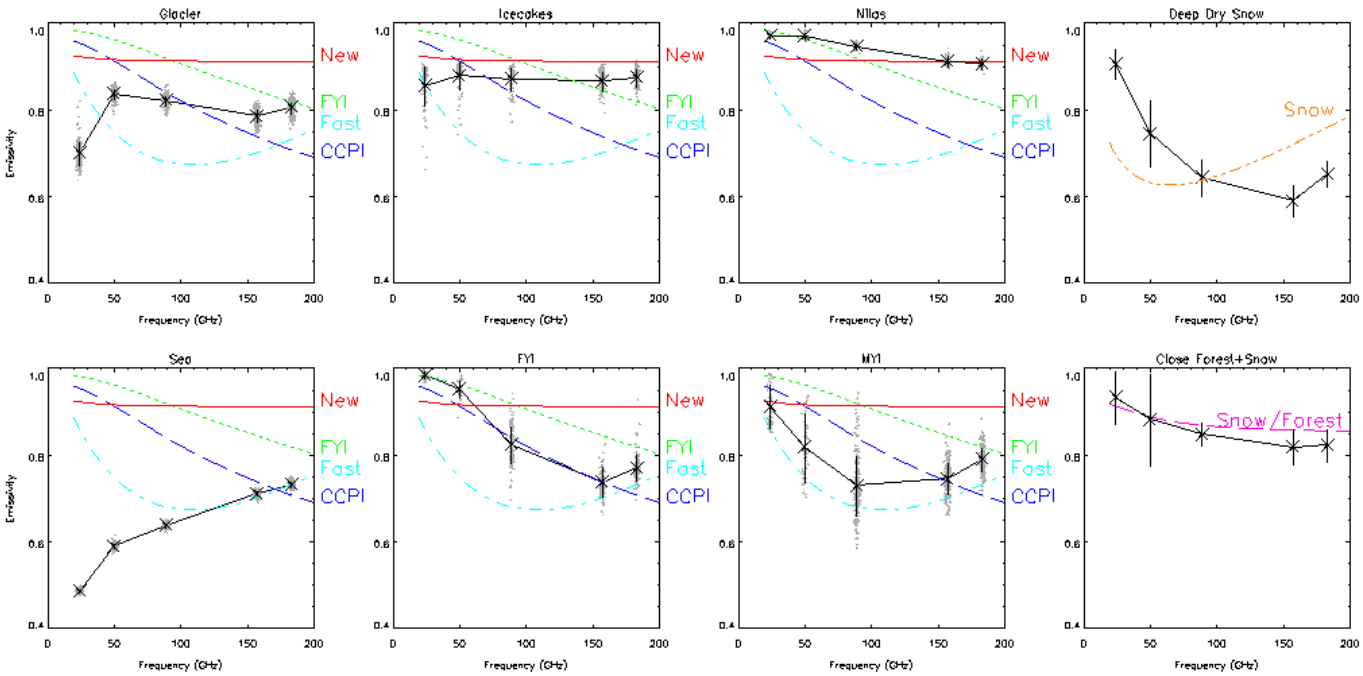

Figure 1 Emissivity for selected POLEX-SEPOR flights calculated from Effective Temperature derived from 183 GHz microwave radiometer measurements. Coloured curves represent emissivity model fitted to previous results for various surface types reported in [2] as indicated by labels.

V. Surface Classification

Different surface types will have different emissivity spectra, depending on the mechanisms responsible for emission and scattering. It is therefore necessary to derive a classification scheme which can be applied in the analysis of flight data and to satellite data for use in Numerical Weather Prediction (NWP). The later may require exploitation of NWP fields or other satellite observations.

From the aircraft some surface types are easily classified by visual observation: open water, different forms of new ice, consolidated first year ice and the presence of forestry on snow covered land. In the last case, it is possible to automate the classification based on albedo measured from the aircraft's pyranometers, as described in [2]. It is also possible to observe clues to indicate the presence of multi-year ice from low-level.

VI. Results

A. Ice Emissivity Spectra

The surface types have been classified manually for two arctic sea ice flights so far. The emissivity was calculated from the nadir observations at each frequency. The resulting emissivity spectra for selected homogeneous periods are shown in Figure 1. The mean and standard deviation of the emissivity is plotted at each frequency. The mean values are connected by a line to illustrate the trend. Each individual observation within each sample is also plotted as a point, with artificial noise applied to the x-axis to illustrate the distribution. Each sample typically covers 10 minutes of flight data (~ 60km).

The emissivity in Figure 1 is calculated using the effective temperature derived from the MARSS' 183 GHz channels. As this is generally higher than the IR skin temperature, the resulting emissivity is correspondingly lower, especially where the ice is older, colder or thicker.

Also shown on the plots in Figure 1 are the emissivity spectra for different surface types, based on the coefficients given for the empirical model presented in [2]. These coefficients are based on previous measurements, concentrated in the Baltic Sea. The highest solid, straight line represents ***Bare New Ice,*** the dotted curve ***First Year Ice***, the dashed curve ***Compact Consolidated Pack Ice***, and the lowest dash-dot curve is ***Fast Ice***. These coefficients were derived from emissivities calculated using an IR skin temperature, which complicates direct comparison.

First Year Ice (FYI) shows a gradual transition along the track of both flights, due to changing physical characteristics of the sea ice or its snow cover. In general, it is best represented by the ***Compact Consolidated Ice*** classification reported for Baltic Sea ice observations in [2], however, the emissivity of FYI consistently increases above 157 GHz.

Further north, there is a gradual transition from First to Multi-Year Ice (MYI). The panel in Figure 1 labelled MYI comprises of a mixture of old floes with well weathered ridges and younger, ridged pack ice more typical of that seen on other flights (FYI). The MYI concentration in this sample was estimated as 80%. It shows a very similar spectrum to the Baltic ***Fast Ice*** and quite different from FYI.

Two different glaciers were over-flown. Their emissivity spectra are quite unlike any other surface type, but depend on the physical structure and temperature gradients within the ice. This implies their emissivity cannot be represented by a global set of coefficients.

B. Snow and Forest Emissivity Spectra

Albedo measurements were used to classify the surface types during the flight on 17 March 2001 near Sodankylä, Finland. Areas where the albedo was greater than 0.75 were classified as ***Deep, Dry Snow***. When the albedo was less than 0.25, it was classified as ***Close Forest + Snow***. These are the same thresholds used in [2].

The resulting emissivity spectra are also shown in Figure 1 at nadir incidence. The dashed curves on these plots indicate the empirical model fitted to observations for each classification based on observations made in the same area at the same time of year in 1997 [2]. The POLEX-SEPOR measurements have quite different characteristics: the emissivity is much higher at low frequencies, and does not increase until 183 GHz. This is due to different physical structure of the snowpack. Although the earlier measurements were classified as dry snow, the temperature had been close to 0 °C a few days earlier and some layers of refrozen snow could have formed below the surface. Such features have a strong impact on the emissivity. This makes it difficult to prescribe a fixed emissivity spectrum for snow. However, again the increase from 157 to 183 GHz is consistent.

The emissivity of the snow covered forest classification is found to be equivalent to a 45:55 mixture of the dry snow measured for this flight and an emissivity of 1, representing dense conifer forest with no snow cover.

C. Emissivity Gradient between 157-183 GHz

The emissivity at 183 GHz appears to be consistently higher than at 157 GHz for all surface types overflown during POLEX-SEPOR. This is illustrated in Figure 2. The residual scatter in this figure is related to the different surfaces overflown on each flight. This frequency range probably represents a transition in the scattering efficiency of particles within the surface media.

This is an encouraging result, as it would allow the emissivity at one frequency to be parameterised in terms of measurements at the other. It may even be possible to retrieve the emissivity at 183 GHz from satellite data.

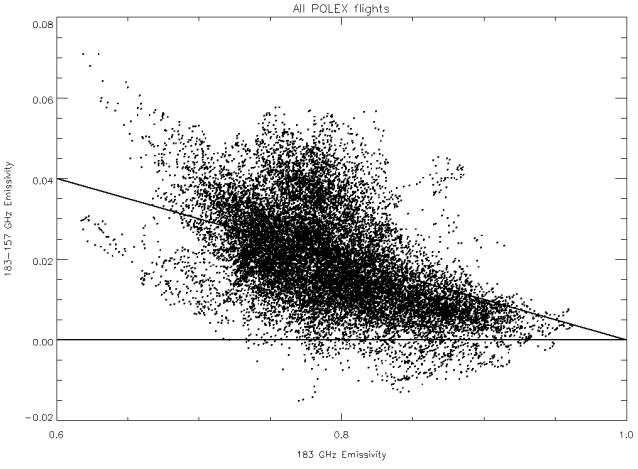

Figure 2 - Emissivity difference 183-157 GHz for all low-level data, smoothed over 10 km. The line shows a 10% difference in reflectivity.

VII. Conclusions and Recommendations

This analysis of data from the POLEX-SEPOR experiment has highlighted a number of problems in the application of the existing fast emissivity model to arctic surface types. In particular, the emissivity of sea ice varies over large scales according to its physical characteristics; and the emissivity of snow is very sensitive to changes in the structure of the snowpack.

These results make it difficult to prescribe an emissivity spectrum to a particular surface type. However, above 100 GHz, the emissivity is less variable and shows a consistent trend. This provides hope that the emissivity in this band could be retrieved from satellite data.

Future analysis will investigate the impact of snow cover on surface emissivity and effective temperature. Emissivity will also be calculated for other view angles and polarisations, including data from other flights.

The empirical model currently used [2] is incapable of representing non-monotonic changes, which are consistently observed in this dataset. The potential of alternate forms of expressing the variation of complex permittivity with frequency will be investigated. Coefficients will then be generated to represent these surfaces in a fast emissivity model.

Acknowledgement

The experiment was partly funded under the Framework Programme V - Improving the Human Research Potential and Socio Economic Knowledge Base under the Transnational Access to major Research Infrastructures from the CAATER programme, contract no. NPRI-CT-1999-00095.

The authors wish to thank the staff of the Norwegian Meteorological Institute (DNMI) for their support and hospitality in Tromsø. The authors would like acknowledge the dedication and support of the aircraft's ground and air crew and the scientists and technicians of the Meteorological Research Flight.

References

[1] N. Selbach, T.J.Hewison, G.Heygster, J.Miao, A.J.McGrath, J.P.Taylor, "Validation of total water vapor retrieval with an airborne millimeter-wave airborne radiometer over Arctic sea ice", Submitted to Radio Science, December 2001.

[2] T.J.Hewison and S.J.English, "Airborne retrievals of snow and ice surface emissivity at millimetre wavelengths", IEEE Trans. Geosci.Remote Sensing, Vol.37, No.4, 1999, pp.1871-1879

[3] T.Hewison, "The design of Deimos: a microwave radiometer with channels at 23.8GHz and 50.3GHz for the UK Met. Research Flight C-130 aircraft", Proc IGARSS'95, 1995, pp.2261-3.

[4] A.J.McGrath and T.J.Hewison, "Measuring the accuracy of a Microwave Airborne Radiometer (MARSS)", Journal of Atmospheric and Oceanographic Tech., Vol.18, No.12, 2001, pp.2003-2012.

[5] P.W.Rosenkranz**,** "Water vapor microwave continuum absorption: A comparison of measurements and models", Radio Science, Vol.33, No.4, pp.919-928, 1998.

[6] Jonathan P. Taylor and Martin D. Glew, "Retrieving land surface temperature and emissivity from ARIES data", MRF Technical Note No.36, 2001, Met Office, UK